Electron Self-Exchange in the Solid-State: Cocrystals of Hydroquinone and Bipyridyl Triazole

Tia E. Keyes,*,† Robert J. Forster,*,‡ Alan M. Bond,§ and Wujian Miao§

Contribution from the School of Chemistry, Dublin Institute of Technology, Kevin Street, Dublin 8, Ireland, School of Chemical Sciences, Dublin City University, Glasnevin, Dublin 9, Ireland, and School of Chemistry, Monash University, P.O. Box 23, Victoria, 3800, Australia

Received November 15, 2000

Abstract: Solid-state voltammetry, spectroscopy, and microscopy studies have been used to probe the proton and electron conductivity within a self-assembled cocrystal, HQBpt. This crystallographically defined material contains 3,5-bis(pyridin-2-yl)-1,2,4-triazole, HBpt, dimers that are π-stacked and hydrogen bonded to 1,4-hydroquinone, H_2Q, in a herringbone arrangement. When deposited onto platinum microelectrodes, the cocrystal exhibits a well-defined voltammetric response corresponding to oxidation of H_2Q to the quinone, Q, across a wide range of voltammetric time scales, electrolyte compositions, and pH values. Scanning electron microscopy reveals that redox cycling in aqueous perchlorate solutions in which the pH is systematically varied from 1 to 7 triggers electrocrystallization and the extensive formation of rodlike crystals. Fast scan rate voltammetry reveals that the homogeneous charge transport diffusion coefficient, D_{app}, is independent of the perchlorate concentration for $0.1 < [ClO_4^-] < 1.0$ M (pH 6.6) at $3.14 \pm 0.11 \times 10^{-9}$ cm^2 s^{-1}. Moreover, D_{app} is independent of the perchloric acid concentration for concentrations greater than approximately 2.0 M, maintaining a value of $4.81 \pm 0.07 \times 10^{-8}$ cm^2 s^{-1}. The observation that D_{app} is independent of the supporting electrolyte suggests that the rate-determining step for homogeneous charge transport is not the availability of charge-compensating counterions or protons, but the dynamics of electron self-exchange between H_2Q and Q. We have used the Dahms−Ruff formalism to determine electron self-exchange rate constants which are $2.84 \pm 0.22 \times 10^9$ and $9.69 \pm 0.73 \times 10^{10}$ M^{-1} s^{-1} for pH values greater than approximately 2.0 and less than −0.3, respectively. Significantly, these values are more than 2 orders of magnitude larger that those found for benzoquinone self-exchange reactions in aqueous solution. These results indicate that hydrogen bonds play an important role in supporting rapid electron transfer. The increase in D_{app} between pH 1.0 and −0.3 is associated with protonation of the HBpt moieties, which triggers a *reversible* change in the material's structure.

Introduction

In sharp contrast to the large number of solution-phase investigations, there have been surprisingly few studies on coupled electron- and proton transfer within H-bonded solid-state materials. Coupled electron/proton-transfer processes play a pivotal role in many biochemical processes.[1,2] For example, in bacterial photosynthesis,[3] and in the respiratory transport chain, an important proton source and sink is a quinone/hydroquinone (Q/H_2Q)-based moiety.[4] Systems of this kind generate a significant transmembrane proton gradient because oxidation of H_2Q to Q triggers the release of two protons. The study of solid-state materials offer significant advantages in this regard, since forces such as intermolecular H-bonding or π-stacking are necessarily weak and disrupted in solution. Two significant advantages are: first, careful studies on biosystems have proven that both the secondary structure and hydrogen bonding play critical roles in dictating the efficiency of long-range electron transfer.[5] Hydrogen-bonded crystalline materials may provide uniquely well-defined model systems in which to probe the effect of distance, reactant orientation, and relative energy separation on mass- and charge transfer. Second, they would reveal the effect of protonation and redox switching on the structure of the assembly, for example, H-bonding interactions might be modulated by redox switching between quinone and hydroquinone forms. Beyond providing an insight into biosystems, information of this kind will underpin key technological advances in the areas of batteries, sensors and "smart" materials for triggered drug release applications.

In this contribution, we report the first investigation into mass- and charge transfer through a solid-state, H-bonded cocrystal. As illustrated in Scheme 1, this material is an electroactive cocrystal formed from 1,4-dihydroxybenzene, H_2Q, and 3,5-bis(pyridin-2-yl)-1,2,4-triazole, HBpt. Solid deposits of this material, HQBpt, on microelectrodes exhibit well-defined electrochemical responses across a wide range of solution-pH values and time scales as well as electrolyte types and concentrations. This cocrystal is an attractive model system for probing coupled electron- and proton-transfer reactions as well as the effects of redox switching and protonation on structure for several reasons. First, the two components are held together by H-bonding and π-stacking interactions to give a well-defined structure, that is, the intersite separation and reactant orientation

† Dublin Institute of Technology.
‡ Dublin City University.
§ Monash University.

(1) Armstrong, F. A.; Heering, H. A.; Hirst, *J. Chem. Soc. Rev.* **1997**, *26*, 169.
(2) Babcock, G. T.; Wikström, M. *Nature* **1992**, *356*, 301.
(3) Huber, R. *Angew. Chem., Int. Ed. Engl.* **1989**, *28*, 848.
(4) Yano, T.; Magnitsky, S.; Ohnishi, T. *BBA-Bioenerg.* **2000**, *1459*, 299.
(5) Gray, H. B.; Winkler, J. R. *Annu. Rev. Biochem.* **1996**, *65*, 537.

10.1021/ja003966j CCC: $20.00
Published on Web 03/06/2001

Scheme 1

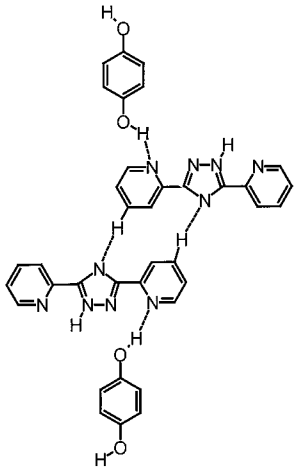

are known from X-ray crystallography. These intermolecular forces are found in many biological systems and play important roles in mediating electron transfer. Second, the hydroquinone is redox active and exhibits proton-coupled redox chemistry.[6] Third, the bipyridyl triazole moieties can be protonated, potentially providing receptor sites for protons ejected when the hydroquinone is oxidized. Fourth, and perhaps most significantly, the cocrystal can provide a compelling insight into the structural effects of oxidizing or protonating the solid deposit.

We have used microelectrodes to probe structural parameters, for example, the fixed site concentration, and dynamic parameters, for example, electron-transfer rates, of the material.[7] An important feature is that the cocrystal shows only a limited solubility even when oxidized. This result is surprising given that the hydroquinone protons are no longer available for hydrogen bonding. However, it appears that the protons ejected during hydroquinone oxidation protonate the pyridine moieties of the HBpt, creating an alternate H-bonding network. This result suggests that the combination of hydrogen bonding and π-stacking can be exploited to direct the formation of solid crystalline assemblies.[8] A striking result is that, depending on the composition of the electrolyte, a rapid electrocrystallization process can be triggered by redox cycling.

We have also probed how electroneutrality is maintained within the cocrystal during redox switching by systematically varying the identity and concentration of the supporting electrolyte. These results reveal that the H-bonded network of the cocrystal facilitates rapid proton conduction, making electron self-exchange between adjacent hydroquinone/quinone couples the rate-determining step. Comparing the self-exchange rate constants for the cocrystal with the corresponding rate constants for hydroquinone in solution provides a direct insight into the effects of distance and reactant orientation on electron-transfer rates. The implications of this work are far-reaching and impact our understanding of electron-transfer processes in materials bound by weak intermolecular forces.

Experimental Section

Chemicals. All chemicals were purchased from Sigma-Aldrich. Hydroquinone, 1,4-dihydroxybenzene was purified via recrystallization from ethanol prior to use, all other reagents were used as purchased. HBpt was prepared as described previously.[9]

Cocrystal of 1,4-Hydroquinone and 3,5-Bis(2-pyridyl)-1,2,4-triazole. The cocrystal was prepared via a technique modified from that described previously.[10] A solution of hydroquinone, (0.1 g, 9×10^{-4} mol) in ethanol (10 cm^3) was added to Hbpt, (0.3 g, 1.4×10^{-3} mol) in ethanol, 10 cm^3, and the resulting tan precipitate was recrystallized from ethanol/water, 2:1. Yield 62%. $^1H_{nmr}$ (CD_3CN); H6: 8.58 (d, 4 H), H5: 7.42 (t, 4H), H4: 7.84 (t, 4H), H3: 8.45 (d, 4H), HQ, H2′,H3′, H5′, H6′: 6.70, (s, 4H). Mp, 228 °C (lit. 228 °C).

Instrumentation. Microelectrodes were prepared using platinum microwires of radii between 2 and 25 μm sealed in a glass shroud that were mechanically polished and electrochemically cleaned as described previously.[11]

In experiments designed to determine the fixed-site concentration, radial diffusion conditions are required, and the thickness of the deposit must be at least 5 times greater than the radius of the microelectrode. To create these thick films, the platinum wire was chemically etched using hot HNO_3/HCl as described by Faulkner and co-workers[12] to create a cavity at the electrode tip. Depending on the etching time, the depth of this cavity was between 5 and 50 μm and had a radius between 1.5 and 5 times that of the platinum wire. This cavity was then packed with the cocrystal. The dimensions of the cavity allow a constrained radial diffusion field to be established within the deposit.

All potentials are quoted with respect to a CH Instruments aqueous Ag/AgCl (saturated KCl) reference electrode. Cyclic voltammetry was performed using a CH Instruments model 660 Electrochemical Workstation. All electrolytes were thoroughly degassed using nitrogen, and a blanket of nitrogen was maintained over the cell during all experiments. All electrochemical measurements were carried out at 22 $\pm$ 2 °C.

In experiments designed to probe homogeneous charge transport under linear diffusion conditions,[13] the solid was transferred from a filter paper onto the surface of the working electrode by mechanical abrasion. This process caused some of the complex to adhere to the electrode surface as a random array of particles. After use, the electrode surface was renewed by polishing with an aqueous slurry of 0.05 μm alumina.

Scanning electron microscopy (SEM) was performed using a Hitachi S-3000N system. For SEM investigations, deposits were formed on 3 mm radius carbon disks. In electrochemical investigations, the modified disks were electrochemically cycled between 0.9 and -0.5 V versus Ag/AgCl, and then the layers were allowed to soak in electrolyte free Milli-Q water for at least 20 min before being rinsed and then dried in a vacuum desiccator overnight. SEM reveals that for all electrolytes investigated, unmodified electrodes do not show any evidence of amorphous or crystalline deposits if similarly treated, that is, the washing procedure effectively removes any excess salt from the electrode surface. Furthermore, deposits which were not electrochemically treated showed no alteration on washing and drying.

Raman spectroscopy was conducted on a Dilor·Jobinyvon·Spex Labram. The exciting 20 mW helium−neon laser (632.8 nm) was focused through a purpose-built electrochemical cell onto the mechanically attached sample on a 2 mm radius glassy carbon electrode surface using a 10× objective lens. The beam diameter when focused is approximately 1 μm, producing approximately 10^6 W cm^{-2} at the sample. Focusing was confirmed by using an imaging video camera. A spectral resolution of 1.5 cm^{-1} per pixel was achieved using a grating of 1800 lines/mm. The applied potential was controlled with respect to a Ag/AgCl reference electrode using a CH instruments model 602A potentiostat.

Electrochemical Quartz Crystal Microbalance experiments were performed on a Elchema EQCM-701 electrochemical quartz crystal

(6) O'Hanlon, D.; Forster, R. J. *Langmuir* **2000**, *16*, 702.
(7) Forster, R. J.; Keyes, T. E.; Bond, A. M. *J. Phys. Chem. B.* **2000**, *104*, 6389.
(8) (a) Etter, M. C. *Acc. Chem. Res.* **1990**, *23*, 120. (b) Aakeroy, C. B.; Seddon, K. R. *Chem. Soc. Rev.* **1993**, 397.
(9) Hage, R.; Dijkuis, A. H. J.; Haasnoot, J. G.; Prins, R.; Reedijk, *Inorg. Chem.* **1988**, *27*, 2185.
(10) Nieuwenhuyzen, M.; Keyes, T. E.; Gallagher, J. F.; Vos, J. G. *Acta Crystallogr*. **1997**, *C53*, 1873.
(11) Forster, R. J.; Faulkner, L. R. *J. Am. Chem. Soc*. **1994**, *116*, 5444.
(12) Faulkner, L. R.; Walsh, M. R.; Xu, C. In *Contemporary Electroanalytical Chemistry*; Ivaska, A., Lewenstam, A., Rolf, S., Eds.; Plenum Press: New York, 1990; p 5.
(13) Bond, A. M.; Marken, F. *J. Electroanal. Chem.* **1994**, *372*, 125.

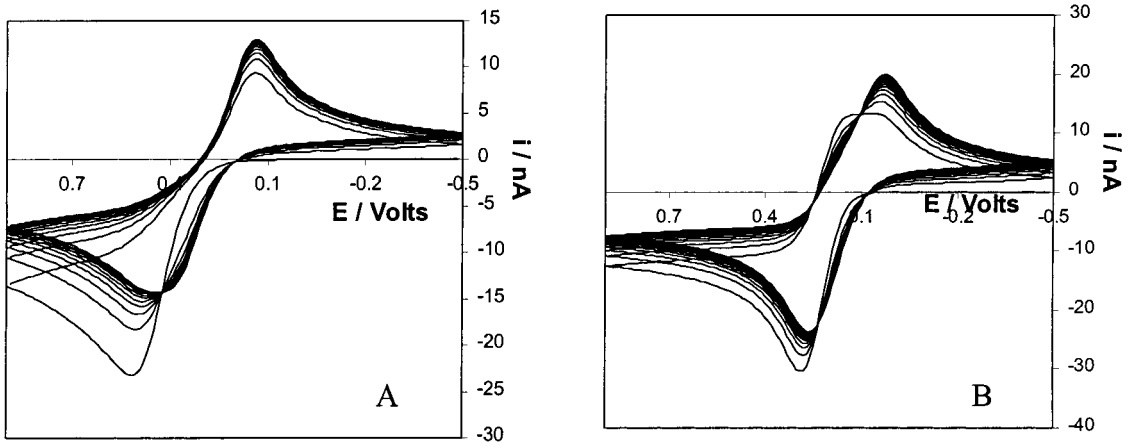

Figure 1. Effect of repeated scanning at 0.5 V s^{-1} on the voltammetric response of an HQBpt deposit that is mechanically attached to a 5 μm radius platinum microelectrode. In (A) the supporting electrolyte is aqueous 0.1 M $NaClO_4$, while in (B) it is 0.1 M $HClO_4$. Anodic currents are down, cathodic currents are up. The initial potential is −0.500 V.

nanobalance as described previously.[14] Ten megahertz gold-coated AT-cut quartz crystals of radius 0.5 cm were employed as the working electrode. The mass sensitivity, ng Hz^{-1}, of the EQCM was determined using electrodeposition of Cu from a 1 mM $Cu(ClO_4)_2$ solution in 0.1 M $HClO_4$. In analyzing the EQCM data for the cocrystal films, we assume that the Sauerbrey equation is valid, that is, that frequency changes associated with viscosity, pressure, and other film properties are negligible.

Results and Discussion

General Electrochemical Properties. As illustrated in Scheme 1, X-ray crystallography reveals that H_2Q exists within the cocrystal in a well-defined microenvironment. The self-assembly of the HQBpt cocrystal is driven by $\pi-\pi$ interactions and extensive three-dimensional H-bonding.[10] There is no direct bonding interaction between molecules that act as linkers in a chain binding HBpt dimers. The electroactive H_2Q in this material provides a compelling opportunity to probe the electronic properties of this material electrochemically.

The solution-phase electrochemistry of hydroquinone, H_2Q, has been extensively studied[15] and is frequently complex in aqueous media where it undergoes a two-electron, two-proton oxidation to produce the neutral product quinone, Q. The proton-coupled electrochemistry makes this reaction highly pH-dependent, and resolving the single two-electron steps with a semiquinone intermediate depends inherently on environmental factors such as the solvent and pH.[16−18]

When first electrochemically cycled, solid deposits often exhibit "break in" phenomena.[19−21] These changes in the voltammetric response are often associated with ion movement and solvation of the redox centers as well as redox induced structural changes. Figure 1A and B illustrate repetitive cyclic voltammograms for mechanically attached layers of HQBpt deposited on a 5 μm platinum microelectrode where the supporting electrolyte is 0.1 M $NaClO_4$ and $HClO_4$, respectively. In both electrolytes, the peak heights alter moderately, by less than 20% over the first 50 cycles. After these initial changes, the peak currents change by less than 5% if repeatedly cycled over a 5-h period. In the case of 0.1 M $NaClO_4$ as supporting electrolyte, the half wave potential for the oxidation reaction, E_{pa}, shifts in a negative potential direction by approximately 110 mV during break-in. This result indicates that it becomes easier to oxidize the film after the first few voltammetric cycles. In contrast, in 0.1 M $HClO_4$, E_{pa} remains constant, but the peak potential for the reduction reaction, E_{pc}, shifts in a negative potential direction, indicating that it is easier to reduce the film after repeated cycling. Bulk electrolysis experiments were performed in order to probe the number of electrons transferred during redox switching and the percentage of the deposit that is electroactive. Typically, 100 μL of a 0.1 mM solution of HQBpt (corresponding to approximately 5.4 μg of material) was drop-cast onto a 3 mm diameter glassy carbon electrode from acetone. The resulting charge measured at +0.800 V was 1.3 mC. With the assumption that two electrons are transferred in the redox reaction, this charge indicates that approximately 70% of the film is electroactive. Given the microcrystalline character of the material vide infra, it seems likely that a significant fraction of the material which does not exhibit a redox response is simply not in direct electrical contact with the electrode.

For $1 \leq pH \leq 7.0$, redox switching of the deposits proceeds as a two-electron process in which the individual electron transfers are not resolved. While these voltammetric responses are well defined, they are irreversible[22] with the peak-to-peak separation, ΔE_p, typically being 200 mV compared to the 28.5 mV anticipated for a simple diffusion-controlled two-electron process. When dealing with the voltammetric responses of solids, it is important to consider the impact of *iR* drop or ohmic loss. The total cell resistance in these experiments is approximately 18 kΩ, which, when coupled with currents of the order of 20 nA, leads to sub-millivolt ohmic losses.[23,24] Therefore, *iR* drop is not the cause of the large ΔE_p observed. Moreover, repeated cycling and bulk electrolysis of the deposits indicate that the redox switching is chemically reversible, that is, the response is not being influenced by a following chemical reaction. Significantly, ΔE_P is independent of the scan rate, υ, at least for $0.1 \leq \upsilon \leq 50$ V s^{-1}, indicating that slow heterogeneous electron transfer across the electrode/deposit

(14) (a) Bond, A. M.; Miao, W. J.; Raston, C. L.; Sandoval, C. A. *J. Phys. Chem. B* **2000**, *104*, 8129. (b) Shaw, S. J.; Marken, F.; Bond, A. M. *J. Electroanal. Chem.* **1996**, *404*, 227.

(15) Patai, S., Chaper, H., Eds. *The Chemistry of Quinoid Compounds*; John Wiley and Sons: London, 1988.

(16) Laviron, E. *J. Electroanal Chem.* **1984**, *164*, 213.

(17) Laviron, E. *J. Electroanal. Chem.* **1984**, *169*, 29.

(18) Binstead, R. A.; McGuire, M. E.; Dovletoglou, A.; Seok, W. K.; Roecker, L. E.; Meyer, T. J. *J. Am. Chem. Soc.* **1992**, *114*, 173.

(19) Bond, A. M.; Fletcher, S.; Symons, P. G. *Analyst* **1998**, *123*, 1891.

(20) Bond, A. M.; Scholtz, F. *J. Phys. Chem.* **1991**, *95*, 7640.

(21) Bond, A. M.; Scholtz, F. *Langmuir* **1991**, *7*, 7640.

(22) Bard, A. J.; Faulkner, L. R. *Electrochemical Methods: Fundamentals and Applications*; Wiley: New York, 1980.

(23) Forster, R. J. *Chem. Soc. Rev.* **1994**, 289.

(24) Forster, R. J. In *Encyclopedia of Analytical Chemistry*; Meyers, R., Ed., Wiley: New York, 1999.

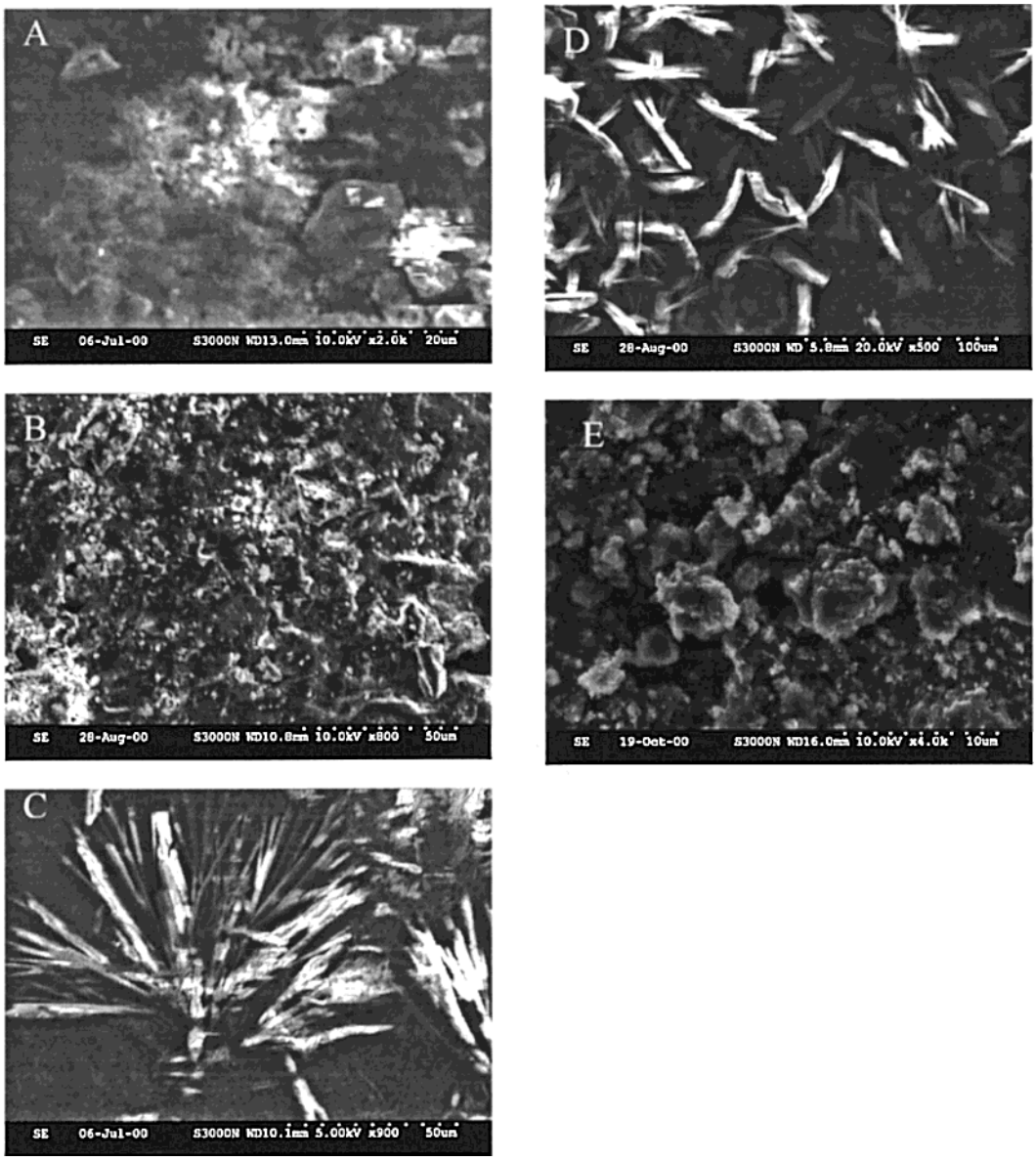

Figure 2. Scanning electron microscopy images of HQBpt deposits on a 3 mm radius pressed carbon disk. (A) As deposited, prior to voltammetric cycling. (B) After exhaustive bulk electrolysis at 0.900 V in 0.1 M $LiClO_4$. (C) After 30 voltammetric cycles at a scan rate of 0.1 V s^{-1} between −0.500 and +0.900 V in 0.1 M $NaClO_4$. (D) After 30 voltammetric cycles at a scan rate of 0.1 V s^{-1} between −0.500 and +0.900 V in 0.1 M $HClO_4$. (E) After 30 voltammetric cycles at a scan rate of 0.1 V s^{-1} between −0.500 and +0.900 V in 3.0 M $HClO_4$.

interface does not contribute to the observed behavior. Rather, the voltammetric response is consistent with changes in structure accompanying the proton-coupled oxidation and reduction processes. This issue of redox-induced morphological changes can be conveniently probed using scanning electron microscopy.

Scanning Electron Microscopy. As illustrated in Figure 2A, after mechanical attachment the deposit consists of a disorganized array of microcrystals, which are predominantly cubic in shape ranging in size from 5 to 50 μm. Figure 2B shows that exhaustive bulk electrolysis of the deposit at an oxidizing potential does not significantly affect the macroscopic structure of the material. Indistinguishable behavior is observed if bulk electrolysis is carried out at a reducing potential. However, as shown in Figure 2C, if the material is subjected to repeated voltammetric cycling, pronounced changes in morphology are observed. Specifically, needlelike crystals about 150 μm long have assembled in rosette formations across approximately 30% of the electrode surface after a single cycle. Further cycling increases the percentage of the electrode surface covered by these needlelike protrusions, up to a maximum of about 70% of the surface by the third or fourth redox cycle. Identical electrocrystallization is observed for deposits cycled in either 0.1 M $LiClO_4$ (pH 6.5) or in 0.1 M $HClO_4$ (pH 1.0), Figure 2D. This behavior agrees with the electrochemical behavior illustrated in Figure 1 where the first few cycles show the most pronounced changes.

At a sufficiently low electrolyte pH, the HBpt moieties are expected to become protonated to yield the pyridinium salt and a 4+ charge per unit cell. This high positive charge would be expected to alter the structure and impede crystallization. As illustrated in Figure 2E, in 3.0 M $HClO_4$ entirely amorphous deposits are observed even after prolonged voltammetric cycling. Consistent with investigations into metal complexes of HBpt,[9] this result suggests that the pK_a of the pyridine sites is less than 1.

Raman Spectroscopy. Raman spectroscopy provides a powerful means of characterizing the electronic and structural changes that occur in solid deposits when their redox state is

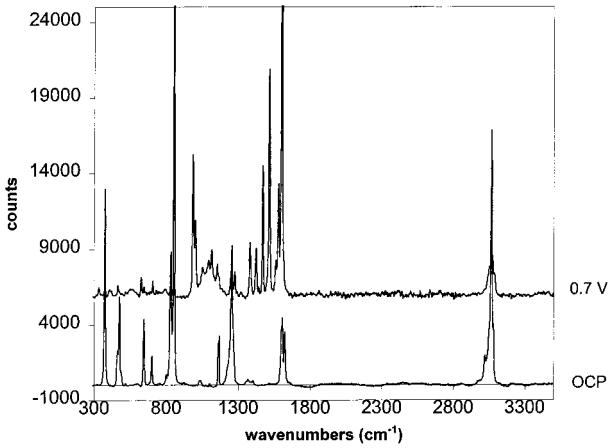

Figure 3. Raman spectra for solid HQBpt deposits on a glassy carbon electrode at open-circuit potential, at +0.700 V. The supporting electrolyte was aqueous 0.1 M $LiClO_4$. The spectra are offset for clarity.

switched. Raman spectroscopy only probes the outer layers of the deposit, thus providing useful information about the extent of redox conversion. Figure 3 shows the Raman spectra of a HQBpt deposit on a glassy carbon electrode at open circuit potential, where the material is fully reduced, and at 0.700 V where it is fully oxidized. The supporting electrolyte is 0.1 M $LiClO_4$. The spectrum changes significantly upon oxidation with bands associated with the hydroquinone at 375, 647, 831, 852, 1254, 1607, and 3067 cm^{-1} being lost and replaced with new features typical of quinone at 1115, 1160, 1397, and 3057 cm^{-1}. The carbonyl stretching frequency is 1600 cm^{-1}, which compares to 1645 cm^{-1} found for a solid deposit of *p*-benzoquinone. The shift to lower frequency suggests that the carbonyl participates in a H-bonding interaction with the adjacent pyridinium moiety. This result suggests that at pHs > 1, the protons ejected when the hydroquinone is first oxidized are retained within the structure by protonating the pyridine groups. Significantly, the Raman response is entirely reversible, suggesting that no new chemical species are permanently formed as a result of oxidizing the deposit.

Fixed Site Concentration and Dynamics of Charge Transport. Voltammetry represents one of the few convenient methods of directly determining the effective concentration of redox centers within solid-state materials.[25−27] The approach exploits the differences in the nature of the diffusion fields that exist at microelectrodes at different experimental time scales, that is, linear versus radial diffusion at short and long times, respectively. It is important to remember that diffusion here refers to transport within the solid, not within the solution phase. Figure 4(a) and (b) show slow scan rate voltammograms for HQBpt where the supporting electrolyte is 0.1 M $LiClO_4$ and 0.1 M $HClO_4$, respectively. In these experiments, a 20 μm deep cavity has been etched in 2 μm radius platinum microelectrode and packed with HQBpt. Under these long time scale conditions, the thickness of the depletion zone is less than 20 μm yet is significantly larger than the electrode radius, and radial diffusion predominates. In both electrolytes a well-defined current plateau is observed that is independent of the scan rate for $1 \leq \upsilon \leq 5$ mV s^{-1}. However, hysteresis is observed between the forward and backward scans. This behavior is consistent with both the high scan rate voltammetry and SEM data presented earlier, both of which suggest that voltammetric cycling changes the

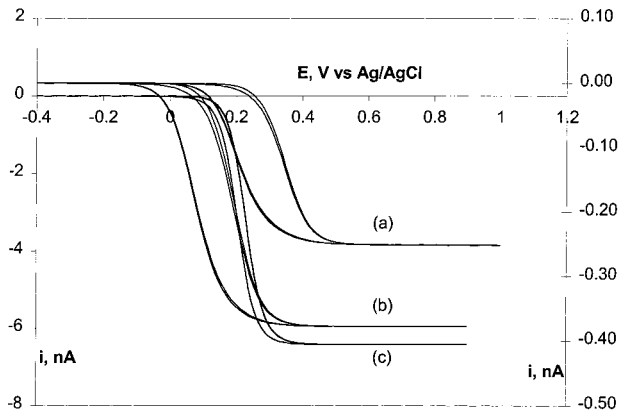

Figure 4. Steady-state voltammograms for HQBpt cocrystals packed within a 20 μm deep cavity etched in a 2 μm radius platinum microelectrode. The scan rate is 1 mV s^{-1}. For (a), (b), and (c), the supporting electrolyte is 0.1 M $NaClO_4$, 0.1 M $HClO_4$, and 3.0 M $HClO_4$, respectively.

structure of the deposit. The hysteresis does not appear to arise because a kinetic process is slow compared to the time scale of the experiment, but because of different structures associated with each oxidation state. Oxidation of the H_2Q moiety results in significant structural change associated with formation of a pyridinum cation in the oxidized state; depending on the sequence of proton- and electron transfers in the oxidation and reduction a scheme of squares, typical of many hydroquinone systems,[15,16] results in hysteresis in the slow scan CV. As shown in Figure 4(c), in 3.0 M $HClO_4$ the oxidation shifts in a positive potential direction by approximately 50 mV which is consistent with a Nernstian response for a reaction in which each electron transfer is coupled to a proton transfer. However, the most striking feature observed in 3.0 M $HClO_4$ is that the extent of hysteresis is dramatically reduced. Under these conditions the protons released on oxidation of the HQ moiety are anticipated to leave the solid, and the state of protonation of the pyridine is unchanged reducing the structural dissimilarities in the two oxidation states.

Although the radial diffusion field is constrained by the cavity, the time-independent steady-state current, i_{ss}, can be approximated by eq 1:

$$i_{ss} = 4nFD_{app}C_{eff}r \qquad (1)$$

where n is a number of electrons transferred, D_{app} is the apparent diffusion coefficient describing homogeneous charge transport through the deposit, C_{eff} is the effective concentration of H_2Q centers within the deposit, and r is the radius of the microelectrode. The steady-state currents observed in Figure 4 indicate that the product $D_{app}C_{eff}$ is approximately 1.6×10^{-12} and 2.4×10^{-12} mol cm^{-1} s^{-1} for 0.1 M $NaClO_4$ and $HClO_4$ electrolytes, respectively.

In contrast to this radial diffusion regime, at short time scales the thickness of the depletion layer is significantly less than the radius of the microelectrode and linear diffusion predominates. Under these conditions, peak-shaped voltammograms reminiscent of those observed for solution-phase species at macroelectrodes are observed. Figure 5A and B show the voltammetric responses for HQBpt deposits in 0.1 M $LiClO_4$ and $HClO_4$ where $0.5 \leq \upsilon \leq 5$ V s^{-1}. The insets of Figure 5 show that the peak current, i_p, increases linearly with increasing $\upsilon^{1/2}$, indicating that the reaction is diffusion-controlled. The slope and intercept of the i_p versus $\upsilon^{1/2}$ plot are the same within experimental error for both oxidation and reduction processes.

(25) Kulesza, P. J.; Faulkner, L. R. *J. Am. Chem. Soc.* **1994**, *115*, 11878.
(26) Whiteley, L. D.; Martin, C. R. *J. Phys. Chem.* **1989**, *93*, 4650.
(27) Winlove, C. P.; Parker, K. H.; Oxenham, R. K. C. *J. Electroanal. Chem.* **1984**, *170*, 293.

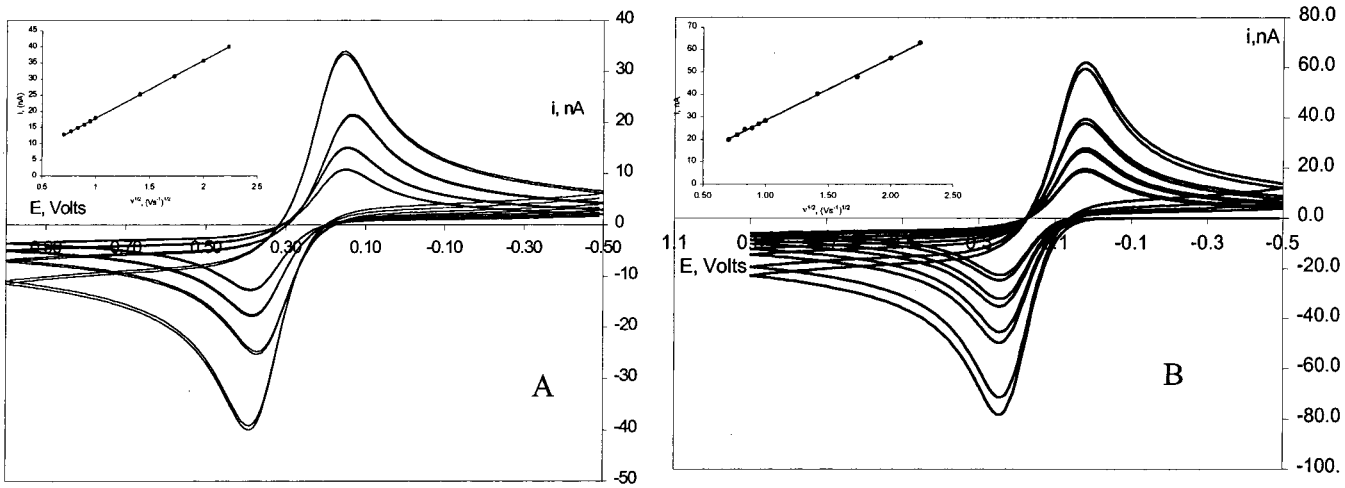

Figure 5. Scan rate dependence voltammetric response for HQBpt mechanically attached to a 5 μm platinum microelectrode in (A) 0.1 M $NaClO_4$ and (B) 0.1 M $HClO_4$. The insets show i_p vs $v^{1/2}$ plots for films under the outlined conditions.

This result is significant since one might expect that, if proton movement was rate-determining, then the rate of proton egress (oxidation) and ingress (reduction) would be different. In a later section, we consider the nature of the rate-determining step by presenting data on the dependence of D_{app} on the concentration and pH of the supporting electrolyte. A second important observation is that, although ΔE_p is clearly larger than that expected for a reversible two-electron two-proton reaction, it is independent of scan rate, indicating that interfacial electron transfer is rapid on the time scale investigated.

Under these circumstances, the peak current, $i_{p,}$ can be described in terms of the Randles−Sevçik equation:[22]

$$i_p = (2.69 \times 10^5) n^{3/2} A D_{app}^{1/2} C_{eff} v^{1/2} \qquad (2)$$

Given that the steady-state current in eq 1 is proportional to $D_{app}C_{eff}$, whereas the peak current of eq 2 is proportional to $D_{app}^{1/2}C_{eff}$, the absolute values of D_{app} and C_{eff} may be determined.[25,28] This approach yields a H_2Q concentration of 0.54 ± 0.12 and 0.88 ± 0.13 M for $NaClO_4$ and $HClO_4$ electrolytes, respectively. These values, especially those found in acidic media, are in satisfactory agreement with the crystallographic value of 0.8 M.

Effect of Electrolyte Concentration on D_{app}. Given that the redox centers are bound within a solid matrix and are therefore immobile, homogeneous charge transport will be limited either by electron hopping or by counterion diffusion/migration. In the case of HQBpt, oxidation of H_2Q is accompanied by proton release to give the neutral quinone product. The protons released may simply diffuse from the solid into solution when the material is oxidized. Alternatively, they may be retained within the solid by protonating the pyridine moieties. Under these conditions, charge-compensating anions would have to move into the deposit to compensate the charge on the pyridinium cations. To observe electron hopping as the rate-determining step, these charge-compensating counterions would have to be freely available within the structure, and D_{app} would depend only weakly on the electrolyte concentration and pH.

Table 1 shows that D_{app} is remarkably insensitive to the $NaClO_4$ concentration, maintaining a value of $3.11 \pm 0.16 \times 10^{-9}$ cm^2 s^{-1} for $0.1 \leq [NaClO_4] \leq 1.0$ M. Also, the D_{app} observed in 0.1 M $HClO_4$, is 2.84×10^{-9} cm^2 s^{-1}, which is identical to within 10% of that found in neutral electrolyte. These data suggest that counterion or proton motion does not limit the rate of charge transport through these deposits. In theory, the electrochemical quartz crystal microbalance (EQCM) can directly probe the changes in the mass of the deposit that accompanies redox switching and allows the identity of the mobile species to be identified.[29] However, studies on these HQBpt deposits are inconclusive because electrocrystallization appears to cause the deposit to become mechanically decoupled from the EQCM. The Raman spectra discussed above suggest that the Bpt moieties are protonated in the oxidized deposit even at near neutral pH. This observation appears reasonable since the high fixed site concentration, 0.54 ± 0.12 M, will trigger the release of a large number of protons within the cocrystal when the deposit is oxidized. The protons released upon oxidation will decrease the pH within the crystal well below the pK_a of the Bpt moieties.[30] Therefore, as illustrated in Figure 6, for $1.0 \leq$ pH ≤ 6.6, it appears that the protons released during oxidation remain within the solid by protonating the Bpt groups. Raman data vide supra support this conclusion, where the quinone is deemed to be H-bridged in the oxidized compound. Perchlorate movement across the crystal/electrolyte interface then maintains electroneutrality. Significantly, the independence of D_{app} on the perchlorate concentration suggests that ion transport is facile and that electron self-exchange between H_2Q/Q pairs of reactants represents the rate-determining step.

Table 1. Dependence of the Apparent Diffusion Coefficients on the Perchlorate Concentration[a]

$[NaClO_4]$/M	$10^9 D_{app}$/cm^2 s^{-1}
0.1	2.95(0.23)
0.2	3.11(0.18)
0.4	3.15(0.13)
0.6	3.09(0.46)
0.8	3.22(0.31)
1.0	3.28(0.19)

[a] Errors are in parentheses and represent the standard deviation on at least three independent deposits.

(28) Forster, R. J.; Keyes, T. E. *Phys. Chem. Chem. Phys.*, submitted for publication.

(29) Ward, M. D. Principles and applications of the electrochemical quartz crystal microbalance. In *Physical Electrochemistry, Principles, Methods and Applications*; Rubenstein, I., Ed., Marcel Dekker: New York, 1995; p 293.

(30) The crystallographic data indicate that the molecular volume of the unit cell is 1040.5 Å^3. This unit cell contains half a hydroquinone moiety, i.e., even ignoring the volume occupied by the atoms, the maximum volume into which a proton is released upon oxidation is 1040.5 Å^3. Therefore, the proton concentration within the fully oxidized cocrystal will be of the order of 1.5×10^6 M, i.e., the pH within the cocrystal will be of the order of −6 when the hydroquinone moieties are oxidized.

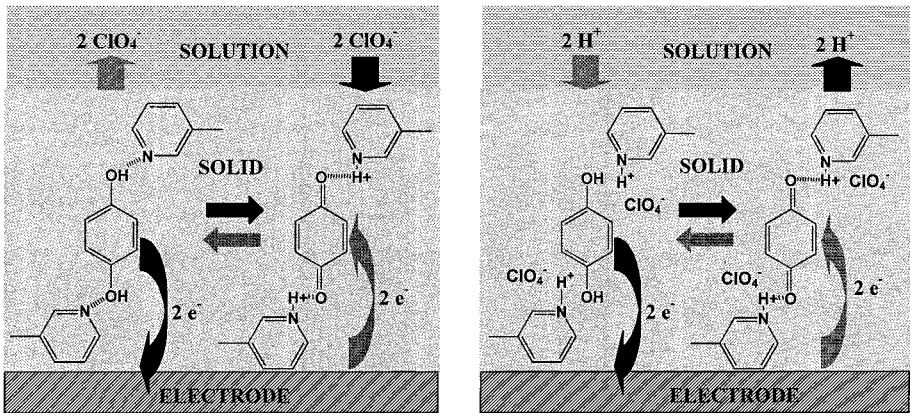

Figure 6. Schematic illustrating the proposed mechanism of charge transport in solid HQ−HBpt, depending on the pH of the media. (a) Between pH 7 and 1 proton transfer is intermolecular with perchlorate anions providing charge compensation. (b) At pH values less than 0.6, the pyridine units are protonated, and the protons released on H_2Q oxidation leave the solid.

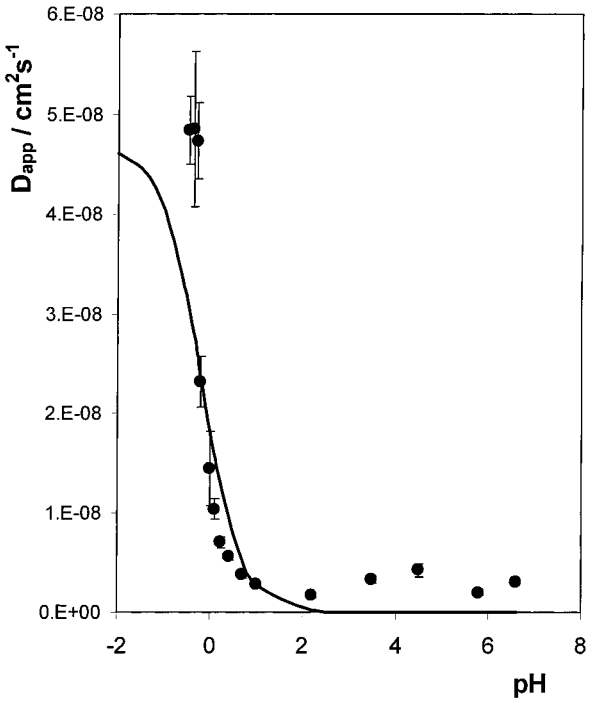

Figure 7. Dependence of apparent diffusion coefficients for HQBpt deposits on the electrolyte pH. The solid line indicates the best fit to the Henderson−Hasselbalch equation. Where error bars are not visible, they are comparable to the size of the symbols.

The voltammetric and SEM data presented earlier suggested that increasing the perchloric acid concentration above 1.0 M can significantly affect the physical structure of the deposits by triggering protonation of the pyridine moieties. Therefore, we have measured D_{app} as the pH of the supporting electrolyte is systematically varied. Figure 7 shows that D_{app} is independent of the electrolyte pH for $1.1 \leq \text{pH} \leq 6.6$. In sharp contrast, between pH 0.7 and −0.2, D_{app} *increases* significantly with *decreasing* electrolyte pH before becoming approximately independent of the solution pH for values lower than approximately −0.3. Given that D_{app} is insensitive to the $NaClO_4$ concentration at pH 6.6, it is unlikely that the availability of perchlorate anions contributes significantly to be observed behavior. Perhaps the most striking result of Figure 7 is its similarity to an acid/base titration curve. The data indicate that the pK_a of the pyridine moieties is -0.25 ± 0.1. The pyridine groups within HBpt show a pK_a of approximately 1.6 when dissolved in aqueous media.[31] This decrease in the apparent pK_a on going from solution to solid states is significant and beyond changes in the local microenvironment is likely to arise because of the hydrogen bonds that exist between the pyridine sites and the H_2Q moieties in the crystalline structure. These hydrogen bonds significantly decrease the basicity of the pyridine nitrogen site since this interaction will place a $\delta+$ charge on the pyridine. As shown in Figure 7, the pH interval over which the cocrystal is converted from deprotonated to protonated states is significantly smaller than that predicted by the Henderson−Hasselbalch equation, approximately 0.7 versus 1.9 pH units. This result suggests that the local microenvironment, for example, dielectric constant, of the pyridine groups within the cocrystal is significantly different from that found in bulk solution. However, the sharp inflection in the titration curve may also arise because the cocrystal is significantly more structurally organized than an aqueous solution. It is perhaps important to emphasize that the differences in D_{app} observed on going from high to low pH are entirely reversible, indicating that any structural changes caused by creating pyridinium sites are not permanent.

As illustrated in Figure 6, the combination of electrochemical, SEM, and Raman data suggest that electron self-exchange represents the rate-determining step for all electrolyte concentrations and pH values investigated. However, at very low solution-pH values the pyridine moieties are protonated, and proton transport across the crystal/electrolyte interface maintains electroneutrality. At these low solution-pH values, protons are freely available, and the cocrystal appears to act as a rapid proton conductor again, making electron self-exchange the rate-determining step. The cocrystal does not dissolve significantly even at low pH values where the deposit is in the reduced state. Under these conditions, the hydroquinone is unlikely to be involved in a H-bonding interaction with the Bpt moieties and, as found in pyridinium polymers, the charge-neutralizing perchlorate anion may play an important bridging role.[32,33]

The Dahms Ruff[34] expression allows the second-order rate constant, k_{SE}, describing the dynamics of self-exchange between adjacent H_2Q/Q moieties, to be determined:

(31) Hage, R., Ph.D. Thesis, University of Leiden, 1991.
(32) Forster, R. J.; Vos, J. G.; Lyons, M. E. G. *J. Chem. Soc., Faraday Trans.* **1991**, *23*, 3761.
(33) Oh, S. M.; Faulkner, L. R. *J. Am. Chem. Soc.* **1989**, *111*, 5613.
(34) (a) Dahms, H. *J. Phys. Chem.* **1968**, *72*, 362. (b) Ruff, I.; Friedrich, V. J.; Demeter, K.; Csillag, K. *J. Phys. Chem.* **1971**, *75*, 3303.

$$D_{app} = D_{phys} + \frac{1}{6} k_{SE} \delta^2 C_{H_2Q} \quad (3)$$

where D_{phys} describes physical diffusion in the absence of electron hopping, C_{H_2Q} is the fixed site concentration of hydroquinone in a fully reduced cocrystal, and δ is the intersite separation between adjacent hydroquinone moieties. Given that the hydroquinones are bound within a solid crystal, D_{phys}, is assumed to be zero. The intersite separation has been estimated from the X-ray crystal structure.[10] The hydroquinones do not interact directly in the cocrystal but are coupled via H-bridges to the π-stacked HBpt moieties at a through-space distance of approximately 9.4 Å. The rate constant for 7 > pH > 1.0 is 2.84×10^9 M^{-1} s^{-1}. Remarkably, this value is approximately 2 orders of magnitude *larger* than that found for *p*-benzoquinone in aqueous media,[35,36] 2.38×10^7 mol^{-1} s^{-1}. This large k_{SE} supports our assertion that electron self-exchange represents the rate-determining step. If D_{app} represented ion or proton transfer, then k_{SE} would have to be significantly larger than 2.8×10^9 M^{-1} s^{-1}. Given that the electron transfer distance within the cocrystal is approximately 9.4 Å and that the Q/H_2Q moieties are linked only through π-stacking and H-bonding interactions, such a large k_{SE} seems unlikely.

The ability of this π-stacked, H-bonded network to facilitate electron transfer agrees with previous reports on protein-based systems where it was demonstrated that hydrogen bridges can efficiently mediate electron transfer.[5,37] In highly acidic media, that is, 3.0 M $HClO_4$, k_{SE} is larger with a value of 9.69×10^{10} M^{-1} s^{-1}. While some of this increase most likely comes from the higher fixed site concentration in acidic media, 0.88 ± 0.13 M, versus that found in neutral 0.54 ± 0.12, it appears that a more favorable electron-transfer pathway exists within the protonated cocrystal. Future investigations will use temperature-resolved measurements of k_{SE} to probe whether differences in the free energy of activation or electronic coupling effects are responsible for the observed behavior.

(35) Chambers, J. Q. In *The Chemistry of Quinonoid Compounds*; Patai, S., Rappoport, Z., Eds., Wiley: New York, 1988; Vol. II, Chapter 12.

(36) Wang, Y. N.; Zhang, X. D.; Liu, Y.; Zhang, Q. Y. *Acta Chim. Sin.* **1999**, *57*, 1114.

(37) Wuttke, D. S.; Bjerrum, M. J.; Winkler, J. R.; Gray, H. B. *Science* **1992**, *256*, 1007.

Conclusions

We have used spectroscopy, microscopy, and electrochemistry to probe, for the first time, mass- and charge transport through a solid deposit of a cocrystalline material, HQBpt, containing 3,5-bis(pyridin-2-yl)-1,2,4-triazole, HBpt, and 1,4-hydroquinone, H_2Q. Oxidation of the hydroquinone moieties between pH 7 and 1 results in an intermolecular proton transfer to the adjacent H-bonded pyridines. Perchlorate transport across the crystal/electrolyte interface is the most likely mechanism by which electroneutrality is maintained within the deposit. However, ion movement appears to be fast, and the apparent diffusion coefficient for homogeneous charge transport, D_{app}, is independent of the perchlorate concentration. By probing the pH dependence of D_{app}, we have determined the effective pK_a of the pyridine moieties within the cocrystal. For all pH and electrolyte concentrations investigated, electron self-exchange limits the overall rate of charge transport through the solid. Between pH 7 and 1 k_{SE} is 2.84×10^9 M^{-1} s^{-1}, and when the pyridine is protonated, it rises to 9.69×10^{10} M^{-1} s^{-1}. These rates are approximately 2 orders of magnitude faster than those observed for *p*-benzoquinone in solution and are attributed to H-bonding and π-stacking interactions responsible for binding the cocrystal. The ability of this π-stacked, H-bonded network to support rapid electron transfer across a through-space distance of approximately 9.4 Å is significant. Future work will focus on determining the extent of electronic coupling between the quinone moieties and comparing this value with that obtained for self-assembled monolayers across the same triazole bridge.[38] Also, these cocrystals represent an interesting medium in which to determine reorganization energies, for example, we plan to determine whether the barrier to electron transfer is dictated by solvent reorganization or structural effects.

Acknowledgment. T.E.K. and A.M.B. acknowledge the financial support of Enterprise Ireland under the International Collaboration Program (IC/1999/006). R.J.F. acknowledges the continuing financial support of the Irish Science and Technology funding agency, Enterprise Ireland. T.E.K. acknowledges the HEA-funded FOCAS project at DIT and DIT for seed funding. The authors thank Professor J. G. Vos, DCU, for synthetic advice.

JA003966J

(38) Forster, R. J.; Vos, J. G.; Keyes, T. E. *Analyst* **1998**, *123*, 1905.